CONVERGENCE OF NEURONAL ACTIVITY PHENOTYPE RESULT FROM SPONTANEOUS OR INDUCED ACTIVITY VIA A COMMON IONIC MECHANISM IN ADULT ISOLATED NEURONS

Rodolfo Haedo
Biological Sciences
Rutgers University
973-353-5080, roculfo@aol.com

Jorge Golowasch
Mathematical Sciences
New Jersey Institute of Technology
973-353-1267, jorge.p.golowasch@njit.edu

CAMS Report 0506-3, Fall 2005/Spring 2006
Center for Applied Mathematics and Statistics

Common ionic mechanism mediates convergence of neuronal oscillatory activity via slow/spontaneous or fast/activity-dependent changes in adult isolated neurons

Rodolfo J. Haedo[1] and Jorge Golowasch[2,1]

[1]Department of Biological Sciences, Rutgers University, Newark, NJ 07102

[2]Department of Mathematical Sciences, New Jersey Institute of Technology, Newark, NJ 07102

Running title: Mechanism of induced and spontaneous oscillations

Corresponding Author:

Jorge Golowasch, Dept. Mathematical Sciences, NJIT, University Heights, Newark, NJ 07102. Phone: 973-353-1267, Fax: 973-353-1007. Email: Jorge.P.Golowasch@njit.edu

Abstract

Neurons exhibit long-term changes in excitability in response to a variety of inputs and perturbations. This plasticity of intrinsic properties is necessary for maintaining proper cell and network activity. The adult crustacean pyloric neuronal network can slowly recover rhythmic activity after complete shutdown resulting from permanent removal of neuromodulatory inputs. We use dissociated stomatogastric ganglion (STG) neurons of the crab *Cancer borealis* as models to study the mechanisms underlying this process. As observed in a different species, STG neurons spontaneously develop a preferred oscillatory activity pattern via gradual changes in excitability, and rhythmic electrical stimulation can regress oscillatory patterns to less excitable states in some cells. However, we show that rhythmic stimulation can more commonly accelerate the emergence of stable oscillatory patterns in cultured crab STG neurons. We find that both spontaneous and activity-induced oscillations correlate with modifications of the same two ionic currents: a Ca^{++} current increase and a high-threshold K^{+} current decrease. Dynamic-clamp experiments confirm that these conductance modifications can explain the observed activity-induced changes. We conclude that the majority of stomatogastric ganglion neurons can become endogenous oscillators and retain this capability into adulthood. However, synaptic interactions or trophic factors may prevent the expression of these oscillations in the intact network. The spontaneous excitability changes observed in isolated neurons may explain the spontaneous recovery of rhythmic activity in the functional network after permanent removal of neuromodulatory input *in situ*.

Keywords: calcium; potassium currents; stomatogastric; excitability; homeostasis; oscillations

Neuronal excitability can undergo long-term changes, which are associated with different forms of learning (Zhang and Linden 2003) and may also play a role in short and long-term memory formation (Daoudal and Debanne 2003; Marder et al. 1996; Zhang and Linden 2003). Modifications of neuronal excitability and intrinsic properties can be elicited by synaptic inputs (Aizenman et al. 2003; Brickley et al. 2001; Leao et al. 2004), electrical stimulation (Cudmore and Turrigiano 2004; Franklin et al. 1992; Garcia et al. 1994; Golowasch et al. 1999a; Li et al. 1996; Turrigiano et al. 1994), development and growth (Spitzer et al. 2002), ionic conductance perturbations (Desai et al. 1999; Linsdell and Moody 1994) and by trauma (Darlington et al. 2002). Regulation of neuronal excitability is thought to be important in the maintenance of stable activity patterns in individual neurons (Davis and Bezprozvanny 2001; Desai et al. 1999; Franklin et al. 1992; Hong and Lnenicka 1995; Li et al. 1996; Linsdell and Moody 1994; Turrigiano et al. 1994) and in neural networks (Galante et al. 2001; Luther et al. 2003; Turrigiano and Nelson 2004). The resulting homeostatic plasticity allows neuronal and network activity to remain within functional limits during their normal operation and in response to perturbations and injury.

Two rhythmic pattern-generating neural networks are found in the stomatogastric ganglion (STG) of crustaceans, the fast pyloric and the slow gastric mill networks (Nusbaum and Beenhakker 2002). The oscillatory activity of all pyloric neurons is conditional upon the presence of neuromodulatory inputs from central ganglia. When these inputs are permanently removed, activity ceases but a stable new activity pattern spontaneously develops within hours to days (Golowasch et al. 1999b; Luther et al. 2003; Thoby-Brisson and Simmers 1998). It has been suggested that this recovery of rhythmic activity occurs via up- and down-regulation of voltage-dependent ionic conductances and the consequent acquisition of oscillatory properties by some of the network components (Golowasch et al. 1999b; Mizrahi et al. 2001; Thoby-Brisson and Simmers 2002).

Although it has been suggested that neuromodulators may have suppressive trophic effects on the excitability of STG neurons (Le Feuvre et al. 1999; Thoby-Brisson and Simmers 1998, 2000)whose effects would be released in dissociated neurons in culture, intrinsic excitability is also affected by patterned electrical activity in isolated STG neurons both in culture (Turrigiano et al. 1994) and *in situ* (Golowasch et al. 1999a).

Changes in activity states of cultured STG neurons can therefore occur spontaneously or by prolonged rhythmic stimulation. The spontaneous changes of activity have been correlated with a decrease of a TEA-sensitive K^+ current and an increase of various inward currents (Turrigiano et al. 1995). However, the conductances changes induced by prolonged rhythmic stimulation that underlie homeostatic activity changes (Turrigiano et al. 1994) have not been identified.

We have studied the spontaneous as well as the activity-dependent recovery of oscillatory activity in adult dissociated crab STG neurons in culture and identified the ionic mechanisms involved in both. We use the dynamic clamp technique to determine if the ionic currents involved are sufficient to produce the observed activity changes.

Materials and Methods

Animals and solutions

Crabs *Cancer borealis* were obtained from local fish markets (Newark, NJ) and maintained in saltwater aquaria at 12° C. The following solution compositions were used (concentrations all in mM): standard *Cancer* saline solution (440.0 NaCl, 11.0 KCl, 13.0 $CaCl_2$, 26.0 $MgCl_2$, 5.0 Maleic acid, 11.2 Trizma base, pH 7.4-7.5); salt supplement solution (743.7 NaCl, 16.4 KCl, 24.7 $CaCl_2$, 50.2 $MgCl_2$ and 10.0 Hepes, pH 7.4); zero Ca^{++}/zero Mg^{++} dissociation solution (440.0 NaCl, 11.0 KCl, and 10.0 Hepes, pH 7.4); barium saline solution (440.0 NaCl, 11.0 KCl, 12.9 $BaCl_2$, 0.10 $CaCl_2$, 26.0 $MgCl_2$, 5.0 Maleic acid, 11.2 Trizma base, pH 7.4-7.5). All chemicals were obtained from Fisher Scientific Co. (Fairlawn, NJ) unless otherwise indicated. The sodium channel blocker Tetrodotoxin, TTX (EMD, Biosciences) was used at 0.1μM.

Cell Dissociation

Crabs were anesthetized by cooling during 15-30 minutes on ice. The foregut was removed, and the stomatogastric ganglia (STG) with a portion of the nerves attached were isolated as previously described (Selverston et al. 1976) in a sterile laminar flow hood. The dissected nerves and ganglia were rinsed 4-5 times in sterile *Cancer* saline containing 0.1 mg/ml gentamicin (MP Biomedicals (Aurora, Ohio). The ganglia were pinned down in sterile Sylgard-lined Petri dishes, incubated in sterile zero Ca^{++}/zero Mg^{++} saline plus 2mg/ml of the proteolytic enzyme Dispase (Gibco, Germany) for 6 hrs at room temperature, and then transferred to an incubator at 12°C overnight in the same solution. Individual somata were then removed from the ganglion by aspiration with glass micropipettes with fire-polished tips. Dissociated neurons were plated individually onto uncoated 35mm plastic Nunclon culture dishes in sterile salt supplement solution diluted 1:1 with sterile Leibowitz L-15 medium (Invitrogen, Carlsbad, CA) and then placed in an incubator at 12°C overnight.

Cells were discarded if they showed blebs protruding from the cell body and if they were not firmly attached to the substrate. Cells with primary neurite and cell bodies

firmly attached to the substrate were found to be the healthiest and produced the most stable recordings.

Electrophysiological recordings

Single (SEVC) or two electrode voltage clamp (TEVC) applied with an Axoclamp 2B amplifier (Axon Instruments, Union City, CA) was used to measure ionic currents. Data were digitized and then analyzed using the pClamp9.0 software (Axon Instruments). Recordings were obtained using Citrate-filled microelectrodes (4M K-Citrate + 20mM KCl). Current injection electrodes had resistances 9-18 MΩ and voltage recording electrodes 15-25 MΩ. The preparation was grounded using an Ag/AgCl wire connected to the bath by an agar bridge (4% agar in 0.6 M K_2SO_4 + 20mM KCl). All experiments were carried out at room temperature (22-24^{o}C).

K^+ currents were separated into 2 components: high-threshold, voltage-gated currents, i_K, activated with 500 ms long depolarizing membrane potential steps from a holding voltage of −40mV, and the voltage-gated transient current, i_A, that was activated with depolarizing steps from a holding voltage of −80mV (Golowasch and Marder 1992; Graubard and Hartline 1991). In crabs the high-threshold component is known to be made up of two conductances, a delayed-rectifier, i_{Kd}, partially blocked by TEA and a Ca^{++}-dependent conductance, $i_{K(Ca)}$, that is completely blocked by 10-20mM TEA and also indirectly by Cd^{++}, which blocks the underlying Ca^{++} current (Golowasch and Marder 1992). The high-threshold currents activated during the i_A activation protocol were removed by subtracting the currents measured from a holding potential of −40mV from those obtained from a holding voltage of −80mV. The hyperpolarization-activated current, i_h, was measured using 4 second long hyperpolarizing pulses from a holding potential of −40mV. The Ca^{++} current, i_{Ca}, was measured with depolarizing membrane potential steps from a holding voltage of −40mV after blocking outward currents. For this, one electrode, filled with 4M K-Citrate + 20mM KCl, was used to record voltage, while the second, filled with 1M TEA + 1M CsCl (12-25 MΩ resistance) was used to inject current. Additionally, 20mM TEA + 0.1μM TTX was added to the bathing

solution. Currents were leak subtracted using the p/n subtraction method included in the data acquisition software, with the holding voltage during leak pulses at −40mV and n=5.

We estimated the conductance of K^+ currents, i_h and i_{Ca} by dividing the current measured at +10, −120 and 0mV, respectively, by their corresponding driving forces, using $E_K = -80mV$, $E_h = -25mV$ and $E_{Ca} = +100mV$ (Golowasch and Marder 1992). In all cases we also determined conductance and midpoint of voltage-dependent activation by fitting conductance vs voltage curves with a Boltzman equation, with conductance calculated by dividing current by driving force (see equations below). i_{Kd} and i_h were measured at steady state, while i_A and i_{Ca} were measured at the peak (25-80ms after pulse onset). To normalize currents they were divided by the current value measured in control at 0mV. We chose this voltage because not all cells could be voltage clamped to levels higher than 0mV; thus, currents measured at 0mV maximized the numbers of cells we could use for our analysis. The leak conductance was measured either as $1/R_{in}$, where R_{in} is the input resistance measured with small hyperpolarizing current steps in current clamp, or as the slope of the I-V curve in the voltage range where no voltage-dependent currents appear to be activated (−40mV to −60mV).

Neurons were allowed to rest for 15-20 minutes after impalement before data acquisition was initiated. Prolonged neuronal stimulation was started only after ionic currents showed stable amplitudes for several minutes, which were then used as control.

Capacitance was determined from the areas of the capacitive transient resulting from 10 ms long hyperpolarizing membrane potential steps from a holding voltage of −40mV to −50mV.

Stimulation protocols

Neuronal activity was altered by applying 500ms long hyperpolarizing current pulses at 0.33Hz, driving neurons to a membrane potential of approximately −120mV. This protocol has been found to be effective in modifying the spontaneous activity of cultured lobster STG neurons before (Turrigiano et al. 1994). Current level was adjusted often during the stimulation period to maintain this level of hyperpolarization. Control

ionic current measurements were recorded in voltage clamp immediately prior to the beginning, and then again after a 45-60 minute stimulation period.

Statistical analysis

SigmaStat (Aspire Software International, Leesburg, VA), Origin (OriginLab, Natick, MA), and CorelDraw (Corel Corp., Canada) software packages were used for statistical and graphical analysis. Analysis of variance (ANOVA) tests were performed using either a standard Two-Way ANOVA or the non-parametric Kruskal-Wallis ANOVA on Ranks for non-normally distributed populations. Results of statistical analysis were considered significant if the significance level P was below $\alpha = 0.05$. All error bars shown and the reported variability around the averages correspond to standard deviations (SD) of the mean.

Dynamic clamp experiments

A NI PCI-6070-E board (National Instruments, Austin, TX) was used for current injection in dynamic clamp experiments. Data acquisition was performed using the Digidata board and pClamp software as described above. The dynamic clamp software was developed by Farzan Nadim and collaborators (available for download at http://stg.rutgers.edu/software.htm) in the LabWindows/CVI software environment (National Instruments, Austin, TX) on a Windows XP operating system. Ionic currents modified by prolonged rhythmic stimulation were recorded in neurons that showed an approximately average effect. They were then fitted with Hodgkin & Huxley-type equations. We used the measured parameters that produced the best fit to reproduce ionic conductances that were then added to or subtracted from a neuron using dynamic clamp (Sharp et al. 1993) adjusting only the maximum conductances to match the effects of rhythmic stimulation.

The equations we used to characterize each ionic current i_X are:

$$i_X = g_{\max X} m_X h_X^q (V_m - E_x)$$

$$\tau_{mX} \frac{dm_X}{dt} = (m_{X\infty} - m_X) \qquad m_{X\infty} = \frac{1}{1 + e^{-(V_m - V_{1/2mX})/s_{mX}}}$$

$$\tau_{hX} \frac{dh_X}{dt} = (h_{X\infty} - h_X) \qquad h_{X\infty} = \frac{1}{1 + e^{-(V_m - V_{1/2hX})/s_{hX}}}$$

where g_{maxX} is the maximum conductance of the current, m is the activation gate, h is the inactivation gate, V_m is the membrane potential and E_x is the equilibrium potential of ion x that each current is specific for. τ_{mX} and τ_{hX} are the time constants with which the m and h gates respectively evolve in time towards their respective steady states $m_{X\infty}$ and $h_{X\infty}$. These steady states are governed each by two voltage dependent parameters $V_{1/2X}$ and s_X that are listed in Table 1. q is an exponent that takes value 1 if the ionic current exhibits voltage-dependent inactivation and value 0 if it does not.

Results

Spontaneous activity changes with time in culture

Our dissociation procedure typically yielded around 20-40% of the 25-26 STG neurons found (Kilman and Marder 1996) in each ganglion and, with careful suction, a relatively long segment of the major neurite could be removed. Figure 1A-C illustrates the morphology of 3 typical neurons with differing neurite lengths immediately after dissociation (Day 0, 1) and 6 days later. By the sixth day in culture some neurons grew wide lamellipodia (Fig. 1A), others tended to grow one or more long processes with smaller lamellipodia extending from the ends (Fig. 1C), while others showed a combination of relatively wide lamellipodia and long processes (Fig. 1B). Any significant outgrowth originated almost exclusively from the neurite stump (Figs. 1B-C) however short it may have been (see Fig 1A). Only very small extensions were sometimes seen growing directly out of the soma (Fig. 1B, Day 6). Figure 1D shows a typical neuron after three weeks in culture, with fine dendrites emerging along most of the major neurite. No obvious correlation was observed between the length of the original neurite and subsequent outgrowth morphology or electrical activity.

Neurons were classified according to the pattern of activity they expressed. Neurons on day 0 were recorded approximately 2 hours after dissociation, time required for cells to begin to attach to the substrate. Three types of electrical activity were readily distinguishable from the first day in culture when the cultured neurons were depolarized with low amplitude current injection: passive (Silent), tonic firing of action potentials (Tonic) or slow oscillations sometimes capped with a burst of action potentials (Bursting). None of the neurons recorded during the initial 10 days in culture expressed spontaneous activity without some depolarizing current and all neurons were tested with depolarizing current steps of various amplitudes. Neurons that responded passively to all depolarizing current levels were classified as Silent. Most neurons (81%) fell into this category on day 0 (see examples on Day 1 in Fig. 1A, B; Fig. 2A). 14% of the neurons showed tonic firing of action potentials on day 0 (Fig. 2A), which we defined as fast, transient depolarizations having a duty cycle ≤ 0.2 (see examples on Day 4 in Fig. 1A)

and that could be blocked with 0.1-1 μM TTX. Duty cycle was defined as the duration of a depolarizing event (action potential or slow oscillation) relative to the period of an oscillation measured at 50% of the maximum oscillation amplitude. A very small percentage (<5%) of the nearly 350 neurons we recorded from expressed bursting activity on day 0 (Fig 2A). Bursting was defined as slow, low amplitude depolarizations having a duty cycle >0.2 (see examples on Day 6 in Fig. 1 A-C) and resistant to TTX treatment. The oscillations recorded on days 4 and 6 of Figure 1B are considered to be at a transition between tonic and bursting states and were classified as bursting.

Figure 2A shows that during days 0-3 in culture the silent state of activity was dominant, but the proportion of bursting neurons steadily increased. The proportion of tonic neurons began to increase at day 3, while the proportion of silent neurons steadily decreased. The proportion of silent neurons continued to decrease throughout the initial 7 days, while that of bursting neurons steadily increased with the exception of day 4. Instead, the proportion of tonically firing neurons seemed to reach a plateau on day 4 (Fig 2A) but were completely absent at 23 day in culture when 87% of the cells expressed either robust bursting or plateau properties (defined by the ability to induce a voltage plateau with a short depolarizing current pulse or to terminate it prematurely with a brief hyperpolarizing current pulse; see top trace in Fig. 1D). Furthermore, in 30% of these neurons excitability had increased enough so that no steady depolarizing current was required to elicit them to burst or to plateau. Plateau potentials were observed in 7/13 (Fig 1D, top panel) while bursting activity was recorded in 6/13 neurons during a steady injection of depolarizing current (Fig. 1D, bottom panel). For the purposes of this figure we have combined bursting and plateau generating neurons into the bursting category. However, when measured at rheobase for the generation of oscillations the average frequency of oscillations of the bursting subpopulation was 1.59 ± 0.52 Hz, while the average oscillation of the plateau generating neurons was significantly lower 0.30 ± 0.20 Hz (P = 0.0005, n = 13, unpaired Student t-test). The rate of change of neuronal activity we observed was slower than that previously observed in cultured lobster neurons (Turrigiano et al. 1995). This may be due to the fact that we incubated our dissociated cells at 12^{o}C instead of 20^{o}C and/or to species differences.

Spontaneous conductance changes with time in culture

To better understand the contributions of individual ionic currents to the activity changes described above, we measured individual ionic currents at different times in culture and estimated their conductance. Figures 2B,C show the evolution of 5 different ionic conductances over up to 10 days in cell culture. Only two of these showed statistically significant changes over that period (Fig. 2B) even after normalizing by the capacitance of the cell: g_{Ca}, which increased by 159% ($P = 0.001$, n = 38), and the high threshold outward current g_K that includes both a delayed rectifier and a Ca^{++}-dependent K^+ current (Golowasch and Marder 1992), which decreased by 54% ($P = 0.047$, n = 65, Fig. 2B). g_{leak} increased by 79% ($P = <0.001$, n = 139, Fig. 2C) but when normalized by cell capacitance the increase was reduced to only 15% and was not statistically significant ($P = 0.777$, n = 32). Thus, the change in leak conductance can probably be explained simply by the growth of the cell, while both g_{Ca} and g_K changes appear to be related to changes in neuronal activity as these changes correlate with the progression from Silent to Tonic to Bursting activity (Fig. 2A). In contrast, g_A and g_h (Fig. 2C) increased by approximately 30% between day 1 and day 10 in culture, but these changes were not statistically significant ($P = 0.654$, n = 62; $P = 0.313$, n = 59, respectively). We did not measure the capacitance in most of the neurons in which g_A and g_h were measured. However, an increase of conductance density of these two currents with age in culture is not likely because the average capacitance during this period increased by the same amount as these conductances (~25%). Furthermore, surprisingly, the increase in capacitance during the first week in culture (for example, c_m on day 1 = 0.437 ± 0.154 nF, c_m on day 7 = 0.548 ± 0.238 nF) was not statistically significant ($P = 0.106$, n = 87). All the above reported statistical tests were performed using the Kruskal-Wallis One Way ANOVA on Ranks.

Activity changes induced by patterned stimulation

The changes in activity patterns and the accompanying conductance changes described above, as well as previous observations in cultured lobster STG neurons

(Turrigiano et al. 1994), suggest that isolated STG neurons follow a set course of spontaneous conductance changes and consequent modifications of activity that may be developmentally predetermined. However, while a neuron may be on a predetermined course to ultimately become a burster, it may also be able to modify its pattern of activity as a function of the inputs it may receive (Cudmore and Turrigiano 2004; Franklin et al. 1992; Garcia et al. 1994; Golowasch et al. 1999a; Li et al. 1996; Turrigiano et al. 1994). We tested this possibility in our crab STG neurons by rhythmically stimulating them with current pulses and measuring possible changes in their patterns of activity. We found that in response to stimulation with hyperpolarizing current pulses the majority of cells (60%) did not change their activity pattern (Fig. 3D) remaining either silent (28%), tonic (12%) or bursting (20%). We refer to this as no change in excitability. Similar to previous observations in lobster STG neurons (Turrigiano et al. 1994) we observed a small set of bursting neurons (10%) that reduced their excitability to tonic firing (Fig. 3B, D). Surprisingly, 30% of the stimulated neurons enhanced their excitability by switching from either silent to bursting (26%, Fig. 3A, D) or tonic to bursting activity (4%, Fig. 3C, D). Silent or tonic to bursting activity changes were accompanied by a slight depolarization of the baseline membrane potential (Figs. 3A, C), while bursting to tonic changes were accompanied by a slight hyperpolarization (Fig. 3B).

In contrast to that shown by Turrigiano et al (1994) we found no consistent correlation of any of these activity changes with the presence of a measurable post-inhibitory rebound (PIR) in these neurons. Fig. 3E shows the voltage changes during the 'beginning' and 'end' of the stimulation period used to induce activity changes. The traces marked A-C correspond to the cells whose results are shown in panels A-C in this figure. The last trace, showing a relatively large PIR capped with an action potential, corresponds to a bursting neuron whose activity did not change with stimulation. In fact, most of the stimulated crab STG neurons shown in Fig. 3 (59%) express no measurable PIR at all (see traces A and C in Fig. 3E). We found that neurons that do not show a change in activity induced by patterned stimulation generate a PIR on average almost twice as large (4.5 ± 7.2 mV, n = 30) as those that do (2.7 ± 3.5mV, n =16), but this difference is not statistically significant (P = 0.363, unpaired Student t-test).

Interestingly, none of the 50 recorded neurons showed a transition from a silent to a tonic (or from a tonic to a silent) pattern of activity, suggesting a lack of sensitivity to patterned stimulation of those currents responsible for the generation of action potentials. In all cases where recordings could be held long enough (2-4 hours) reversal was always significantly slower than the induction phase and almost always partial. We rarely observed a complete reversal of these effects. Figures 3B and C show the only two examples (of 28 cases) we obtained of complete reversal of activity, and in both it took approximately 2 hours to complete.

It is important to note that the capacity for neurons to regulate activity in an activity-dependent manner did not appear to be related to the age of the neurons in culture but rather to their activity state at the time of stimulation. A similar fraction (40%) of "young" neurons (ages 1-4 days in culture) and "old" neurons (31%, ages 5-8 days in culture) could be induce to change their state of activity. However, most stimulated tonic (average age = 5.3 days) and bursting (average age = 3.5 days) neurons were older than stimulated silent (average age = 1.1 days) cells simply because of the spontaneous progression in activity observed in culture (Fig. 2A).

Within the relatively simple activity pattern categories we have classified these neurons into, there is a wide range of variability in terms of action potential frequency, duration and amplitude, slow wave oscillation frequency and amplitude, threshold current required to elicit patterns of activity, etc. We reasoned that this variability may be related to the expression of large, variable amplitude outward currents (Golowasch et al. 1999a) and that reducing their amplitude may uniform the activity patterns and reveal a more consistent effect of rhythmic stimulation on neuronal activity. When outward K^+ current amplitudes were reduced with 20mM TEA in the bath we did indeed observe a reduction in the variability of the activity states (Fig. 4). All neurons before stimulation were either silent (Fig 4A, Control, n = 6/15) or oscillated with plateau-like depolarizations (Fig. 4B, Control, n = 9/15). When these neurons were rhythmically stimulated 100% of the initially silent neurons developed slow and large amplitude oscillations (Fig. 4A, After Stim) and, as shown in Figures 4B (After Stim) and 7B (left panels), 100% of the initially oscillatory neurons increased the duration of the slow depolarizations by 83% from 319 ±

138msec to 584 ± 369msec (P = 0.030, n = 9), increased their amplitude by 40% from 24.4 ± 14.3mV to 34.1 ± 14.2mV (P < 0.001, n = 8), and also increased their oscillation period by 170% from 473 ± 314msec to 1284 ± 936msec (P = 0.046, n = 6, unpaired Student t-test). These changes, together with the fact that a large fraction of the stimulated neurons were induced to switch their activity from either silent or tonic firing to oscillating in response to prolonged patterned stimulation (Fig. 3D), indicate that these neurons increase their excitability with patterned stimulation (from either silent, tonic firing or weak bursting to robust bursting) under these conditions, and frequently also increase their excitability in normal saline conditions (Fig. 3A, C). This can be interpreted as a homeostatic mechanism for the long-term recovery of oscillatory properties. However, once bursting is achieved, a certain degree of flexibility remains and neurons can revert to tonic (but not to silent) activity depending on the intrinsic properties of the cell and the properties of the input.

Conductance changes induced by patterned stimulation

In those neurons in which an alteration of activity was induced by prolonged modification of their spontaneous activity we observed a statistically significant decrease in high threshold K^+ conductance recorded at +10mV in normal saline of approximately 45% (0.58 ± 0.07μS before stimulation, 0.31 ± 0.04μS after stimulation, P = 0.005, n = 6, paired Student t-test). In those neurons in which the activity was not modified no change in outward conductance was observed (0.65 ± 0.17μS before stimulation; 0.68 ± 0.15μS after stimulation, P = 0.375, n = 6, paired Student t-test; Fig. 3F). These results are consistent with an increased excitability of those neurons sensitive to prolonged stimulation as would be expected for neurons that switched activity from a silent or tonic pattern to a bursting pattern (Fig. 3A, C). These results appear to be inconsistent with the reduced excitability we saw in a small subset of stimulated neurons (12%, Fig, 3D); however, see dynamic clamp results below.

STG neurons *in situ* (Golowasch and Marder 1992; Graubard and Hartline 1991) and in culture (Turrigiano et al. 1995) express large outward currents dominated by a TEA sensitive $i_{K(Ca)}$. In cultured STG neurons 20mM TEA eliminates 84 ± 6% (n = 6) of

the total high-threshold outward current. In contrast with the complete block of $i_{K(Ca)}$ by TEA *in situ* (Golowasch and Marder 1992; Graubard and Hartline 1991), TEA does not completely block $i_{K(Ca)}$ in cultured STG neurons. $i_{K(Ca)}$ constitutes approximately 20% of the outward current recorded in 20mM TEA (defined as the current additionally blocked by 200μM Cd^{++}; the high-threshold current remaining in the presence of Cd^{++} corresponds to a delayed rectifier current, i_{Kd}). In the presence of 20mM TEA we observed that prolonged patterned stimulation induced a significant reduction of the outward current over their entire voltage activation range ($P < 0.001$, n = 6, Two-way ANOVA, Fig. 5A) but with no apparent effect on the voltage-dependence of activation (Fig. 5A; $V_{1/2}$ before stimulation = −9.4 ± 17.6mV, $V_{1/2}$ after stimulation = −10.4 ± 14.7mV, $P = 0.900$, n = 6, paired Student t-test). Because this current is maximally activated at voltages above 0mV, we estimated the maximum conductance from the averages of currents measured at +10mV. Before stimulation the estimated maximum conductance was 0.12 ± 0.06μS, which decreased by a statistically significant 22% to 0.09 ± 0.06μS ($P = 0.022$, n = 7, paired Student t-test). In the absence of specific K^+ current inhibitors these data suggest that most of the spontaneous and stimulation-induced changes of the high-threshold K^+ current could be attributed to $i_{K(Ca)}$ since 87% of the total i_K corresponds to $i_{K(Ca)}$, as defined by K^+ current blockade with Cd^{++} (Golowasch and Marder 1992), and 13% to a delayed rectifier K^+ current. Thus, the 45% stimulation-induced reduction in the total K^+ current that we observe cannot be accounted for by effects on the delayed rectifier only. Furthermore, because we observe a stimulation-induced reduction of 22% of the remaining total outward current in the presence of 20mM TEA, and 20% of that current can be further blocked with Cd^{++} (and thus corresponds to $i_{K(Ca)}$), we conclude that an effect of rhythmic stimulation exclusively on $i_{K(Ca)}$ is in principle sufficient to account for all our observations of activity-dependent effects on outward currents.

We isolated i_{Ca} as described in Methods (Fig. 5B). Stimulation for as little as 15 minutes induced a marked increase in i_{Ca} (Fig. 5B). Figure 5B also shows the current-voltage relationship before (Control) and after rhythmic stimulation of STG neurons. A statistically significant increase over the voltage range of −20 and +30mV is observed ($P = 0.020$, n = 7, Two-way ANOVA), with the peak conductance measured at +10mV

growing 2.5 fold from 0.014 ± 0.031μS to 0.036 ± 0.031μS. (P = 0.046, n = 7, paired Student t-test). We observed no effect of stimulation on the voltage dependence of activation of this current (Fig. 5B; $V_{1/2}$ before stimulation = −2.5 ± 10.0mV, $V_{1/2}$ after stimulation = −5.5 ± 30.2mV, P = 0.099, n = 7, paired Student t-test).

In contrast with the effect on i_K and i_{Ca}, the leak conductance showed no change in conductance in these experiments (0.004 ± 0.003μS before stimulation, and 0.005 ± 0.002μS after stimulation, P = 0.712, n = 7, paired Student t-test). Leak conductance was determined in these experiments from the current changes elicited in response to the voltages steps from −40 to −50 or −60mV shown on the I-V curve of Figure 5A. Additionally, the transient i_A current (measured in TEA to minimize other K^+ currents) is completely unaffected by patterned stimulation in cultured crab STG neurons (Fig. 5C, P = 0.944, Two-way ANOVA over the activation range: −40 to +30mV). The average peak conductance g_A measured at +10mV was 0.42 ± 0.17μS (n = 7).

The hyperpolarization-activated current was not affected by patterned stimulation: the maximum conductance measured at −120mV was 0.015 ± 0.007μS before stimulation, and 0.018 ± 0.010μS after stimulation (P = 0.140, n = 8, paired Student t-test).

Role of calcium influx in activity-dependent regulation of conductances

The conductance changes reported above most likely occurred in response to the experimentally imposed activity pattern and were not due to effects of the electrode-filling solutions (K-citrate, K_2SO_4 or TEA·Cl + CsCl) or of different bathing solutions (TEA, TTX, Cs^+), and occurred in the absence of any known growth factors or neuromodulators. For activity to be responsible for these changes, neurons need to be able to detect changes in patterns of activity. A plausible candidate for such a sensor of activity is intracellular Ca^{++} (Bito et al. 1997; De Koninck and Schulman 1998; Liu et al. 1998; Schulman et al. 1995). Indeed, in our neurons the only conditions that block these effects are those that interfere with Ca^{++} influx. Figure 6A shows an inward current that shows virtually no inactivation when Ca^{++} in normal saline is replaced with Ba^{++}. With Ca^{++} influx thus minimized, no change in the amplitude of the inward current now carried

by Ba^{++} (Control) was observed in response to prolonged patterned stimulation (After Stim, Fig. 6A). No significant changes were recorded over the voltage-dependent activation range (−30 to +30mV) of this current ($P = 0.668$, n = 5, Two-way ANOVA). Similarly, when i_{Ca} was blocked with 200μM Cd^{++} the small remaining outward current, predominantly i_{Kd}, showed no significant change over its voltage range of activation due to patterned stimulation (Fig 6B, $P = 0.973$, n = 5, Two-way ANOVA).

Dynamic clamp experiments

The effects of prolonged stimulation on voltage-dependent currents and neuronal activity only partially reversed during the time we could maintain the recordings (2-4 hours). To verify if the spontaneous and stimulation-induced conductance changes (i_K decrease and i_{Ca} increase) are indeed sufficient to account for the observed alterations in neuronal patterns of activity, we introduced negative or positive outward and inward conductances with dynamic clamp. We fitted with Hodgkin & Huxley-type equations the high threshold outward current difference, and separately the Ca^{++} current difference of neurons sensitive to patterned stimulation in normal saline. For these fits we chose neurons that responded to patterned stimulation with high threshold outward and Ca^{++} current changes close to the population average. The best fit to the outward current could be obtained with two conductance components, one transient (gKtr) and one sustained (gKst), while the Ca^{++} current could be fitted well with a single component (gCa). The conductance parameters thus obtained and used for our dynamic clamp experiments are given in Table 1. Because the voltage dependence of these currents does not appear to be affected by patterned stimulation we modified only the maximum conductances to mimic the changes observed on these two currents. Fig. 7A shows the results of one such experiment on naïve unstimulated neurons recorded in normal saline. Activity was elicited by small depolarizing current injections. Conductance values indicated above the arrows correspond to the maximum conductance values of each dynamic clamp current. Many different patterns of activity could be produced by relatively small changes of the maximum conductance values, which depended on the particular neuron used (Fig. 7A). However, we could repeatedly induce bursting activity by reducing the outward currents (negative conductance) and/or increasing the inward current (positive conductance, Fig

7A, top and middle panels). It was relatively easy to also find combinations of maximum conductance values within the range of the spontaneous or stimulation induced conductance changes described before that could produce tonic firing in a neuron that was originally bursting (Fig 7A, bottom panel). Figure 7B shows in more detail that some properties induced by prolonged rhythmic stimulation can not only be mimicked by adding g_{Ca} and subtracting g_K but also reversed by subtracting g_{Ca} and adding g_K after they were induced by stimulation. Before prolonged rhythmic stimulation was started the neuron shown in Fig. 7B (top left) was induced to produce slow large amplitude oscillations by bathing it in 20mM TEA. Adding g_{Ca} and subtracting g_K with dynamic clamp increased the amplitude and slightly decreased the frequency of bursting (Fig. 7B, top-right). A similar but more pronounced effect was later observed after rhythmically stimulating the neuron for 20 minutes with dynamic clamp discontinued. Finally, the enhanced oscillation amplitude and reduced oscillation frequency induced by rhythmic stimulation was partially reversed by subtracting g_{Ca} and adding g_K with identical levels as used immediately before to induce the changes with dynamic clamp (Fig. 7B, bottom right).

Discussion

Long-term regulation of the intrinsic properties and neuronal excitability can play a key role to maintain activity patterns of single neurons and networks within stable and operational ranges in response to a variety of perturbations (Davis and Bezprozvanny 2001; Desai et al. 1999; Franklin et al. 1992; Galante et al. 2001; Hong and Lnenicka 1995; Li et al. 1996; Linsdell and Moody 1994; Luther et al. 2003; Turrigiano et al. 1994; Turrigiano and Nelson 2004). Here we have used adult cultured stomatogastric ganglion neurons of the crab *C. borealis* to identify mechanisms that may play a role in the recovery and stabilization of the activity of the pyloric network after strong perturbations. Specifically, we find that the regulation of the same two ionic currents (i_K and i_{Ca}) is called into play during the spontaneous regulation of activity after dissociation and during the activity-dependent changes induced with prolonged stimulation. We also find that excitability can not only be reduced by patterned stimulation as has previously been reported (Turrigiano et al. 1994), but can also be heightened with the same type of stimulation, an increase in excitability being 3 times more common than a reduction in crab than in lobster neurons. Finally, our dynamic clamp experiments confirm that the regulation of these two conductances is sufficient to produce all the activity pattern changes we observe in cultured crab STG neurons.

Spontaneous activity changes

The progressive decrease in the proportion of silent STG neurons in primary culture and the increase in the proportion of neurons expressing tonic and, later, mostly oscillatory activity suggests a predetermined tendency to oscillate (see also Turrigiano et al. 1995). After several weeks in culture nearly half of the neurons express fast oscillations whose average frequency strongly resembles the bursting of pyloric neurons while the other half express slow oscillations remarkably similar in frequency to that of the gastric mill activity (Fig. 1D, Bartos et al. 1999; Nusbaum and Marder 1989). Approximately one half of the crab STG neurons are pyloric and one half gastric mill network neurons (Nusbaum and Beenhakker 2002). This nearly 50-50 distribution of neurons expressing pyloric- or gastric-like activity in culture suggests the possibility that

specific STG neurons are fated to oscillate at characteristic high (pyloric) or low (gastric) frequencies.

Pyloric network neurons can behave as oscillators when acutely isolated from the network but, with the exception of the single pacemaker AB neuron, all oscillate irregularly (Bal et al. 1988). These oscillations occur only when neuromodulatory inputs to the STG are intact (Nusbaum and Beenhakker 2002). In the absence of this neuromodulatory inputs all STG neurons, including the AB neuron, lose the ability to oscillate (Bal et al. 1988). Our results and those of Turrigiano et al (1995) indicate, however, that all STG neurons in time evolve robust oscillatory activity when isolated from network and from neuromodulatory influences.

In our culture conditions neuromodulators are completely absent and the recovery of rhythmic activity of isolated STG neurons is reminiscent of the recovery of rhythmic activity in the intact pyloric network after the permanent removal of neuromodulatory inputs (Luther et al. 2003; Thoby-Brisson and Simmers 1998). This latter recovery in lobster is accompanied by the development of oscillatory properties by some pyloric network neurons within a few days (Thoby-Brisson and Simmers 2002). Thus, the acquisition of oscillatory properties we and others (Turrigiano et al. 1995) see in isolated STG neurons in culture provides a plausible mechanism for the recovery of rhythmic activity in the network. The pyloric network is driven by a single AB pacemaker neuron (Miller and Selverston 1982). The gastric mill network instead generates oscillations dependent on network interactions (Nusbaum and Beenhakker 2002). It is an intriguing possibility that the gastric mill network may generate oscillations in a "pacemaker-driven" fashion when chronically deprived of neuromodulatory input.

Two hypotheses (still not tested) may explain the suppression of endogenous oscillatory properties in neurons within the intact STG. First, oscillatory properties are suppressed by neuromodulators exerting trophic effects (Le Feuvre et al. 1999; Thoby-Brisson and Simmers 2000). Second, activity itself regulates the expression of endogenous oscillatory properties (Golowasch et al. 1999b; Turrigiano et al. 1994). Our results are consistent with both hypotheses. In the intact network neuromodulators may somehow suppress the expression of endogenous oscillatory properties in most neurons.

Once this input is eliminated (by cell dissociation or by removal of neuromodulatory input *in situ*) constraints on the expression of these properties are removed and oscillatory activity can be expressed by up- and down-regulation of ionic currents such as those characterized in this work and those characterized previously by (Turrigiano et al. 1995). The possibility that the emergence of oscillatory properties may be developmentally determined does not preclude that activity itself may also regulate neuronal electrical properties (Desai et al. 1999; Golowasch et al. 1999a; Liu et al. 1998).

Activity-dependent effects

Our results show that isolated STG neurons are sensitive to prolonged rhythmic stimulation. Neurons displaying either silent or tonic firing activity can be induced to oscillate, while neurons that show bursting activity remain able to switch between bursting and tonic firing (but not bursting to silent) states (Fig. 3).

The large variability of the effects on activity of prolonged stimulation (Fig. 3D) may be partly due to the heterogeneity of our sample of (unidentified) neurons. However, when outward currents are reduced in the presence of TEA 100% of the stimulated neurons increased their excitability (Fig. 4). Furthermore, all neurons in which outward currents were measured in the presence of TEA showed a decrease in the remaining i_K and all those neurons in which i_{Ca} was measured showed an increase in conductance. The homogeneity of these trends, although variable in their extent, suggests to us that all STG neurons, irrespective of cell type, can regulate their excitability in an activity-dependent manner and via the same ionic mechanism, namely by down-regulation of a high-threshold outward current and an up-regulation of a Ca^{++} current. Experiments with identified STG neurons will confirm this conclusion.

Ionic mechanism of activity regulation

Only two ionic currents appear sensitive to prolonged patterned stimulation in dissociated *C. borealis* STG neurons, a Ca^{++} current and a high-threshold K^+ current. The same two currents are responsible for the spontaneous changes of activity seen in these

neurons. It has previously been shown in cultured lobster STG neurons that, in addition to these currents, changes in two Na^+ currents also correlate with spontaneous changes of activity from silent to tonic firing but that only i_{Ca} continues to increase as neurons become bursters (Turrigiano et al. 1995). Additionally these authors observed a drastic reduction in the transient A current as neurons transition between silent, tonic and bursting states. We cannot exclude the participation of Na^+ currents in cultured crab STG neurons. The fact that tonic firing is completely absent in all neurons after 3 weeks in culture and that silent cells can never be induced to fire action potentials suggests that Na^+ currents in crab STG neurons, like their lobster counterparts, may not be subject to long-term up-regulation or to activity-dependent regulation, but perhaps only spontaneously and transiently during the first few days in culture. In contrast, with the findings by Turrigiano et al (1995) we seen no change in the transient outward A current at any time in culture (Fig. 2C), and also no changes in i_A are induced by prolonged stimulation. Our lack of effects of prolonged hyperpolarizing stimulation on i_A is also consistent with the lack of effects of similar stimulation on this current in two different pyloric neurons *in situ* (Golowasch et al. 1999a). However, *in situ* stimulation of these same cells did also not affect the high-threshold K^+ currents that we see affected in our STG cultured neurons (Golowasch et al. 1999a). It is possible that *in situ* the high-threshold K^+ currents sensitive to stimulation represents a small current relative to the total current and thus activity or total conductance changes could not be unambiguously discerned.

The approximately 2.5-fold stimulation-induced i_{Ca} increase was achieved with approximately 60 minutes of stimulation. i_{Ca} increases spontaneously also by approximately 2.5-fold but over 4 days in culture (Fig. 2B). Similarly, the high threshold K^+ conductance was reduced by 45% in normal saline with rhythmic stimulation but changes spontaneously by only 25% over 10 days in culture. Thus, although the same currents appear targeted during spontaneous and induced activity changes, these effects may occur via two different, but probably overlapping pathways. Slow, spontaneous changes may predominantly require gene transcription and protein synthesis, similar to the transcription requirement for spontaneous but slow pyloric activity recovery in the intact pyloric network after the permanent removal of neuromodulatory inputs (Thoby-

Brisson and Simmers 2000). In contrast, faster stimulation-induced activity changes may involve ion channel activation via some form of post-translational modification.

Our dynamic clamp experiments confirm that an increase in Ca^{++} and a decrease in K^+ conductances are sufficient to explain the observed activity changes. We were able to induce a switch from either silent or tonic firing to bursting activity by modifying the same conductances that we showed to be affected during spontaneous activity changes and by patterned stimulation (i_{Ca}, i_K) within the ranges observed physiologically (Fig. 7A). Although increasing i_{Ca} with dynamic clamp always increased the capacity of neurons to burst, it is important to remember that this current is not a Ca^{++} current in the biological sense since no Ca^{++} influx occurs. An increase in Ca^{++} influx due to an augmented biological i_{Ca} will be accompanied by an increase in $i_{K(Ca)}$, which can reduce the excitability of a neuron and thus induce tonic firing. However, even a dynamic clamp-reduced K^+ current in a background of high i_{Ca} can switch a bursting to a tonically firing neuron (Fig. 7A, bottom panels), similar to 41% of our rhythmically stimulated bursting neurons (Fig. 3C, D). Consistent with our observations of stimulation-induced activity changes, we could never induce tonic firing in silent cells by manipulating i_{Ca} and i_K.

Our observations suggest that changes in Ca^{++} and high-threshold K^+ currents, both spontaneously or induced by rhythmic stimulation, likely play a central role in homeostatic recovery of rhythmic function in the decentralized pyloric network of the crab STG. Decreases in K^+ currents as a result of decreased neuronal drive are common to most if not all systems in which a homeostatic recovery of excitability can be identified (Zhang and Linden 2003). Although sometimes Na^+ currents are also affected (Desai et al. 1999; Mee et al. 2004), more commonly Ca^{++} currents are strengthened due to decreased activity (Chung et al. 1993; Garcia et al. 1994; Su et al. 2002) or reduced due to enhanced neuronal activity (DeLorme et al. 1988; Franklin et al. 1992; Hong and Lnenicka 1995; Li et al. 1996).

Intracellular signaling

We show that activity-dependent Ca^{++} and K^+ conductance changes depend on Ca^{++} influx into these cells. Ca^{++} influx appears to be crucial also in other systems in mediating activity-dependent conductance and activity changes during development

(Spitzer et al. 2002) and in the adult (Zhang and Linden 2003). Several possible Ca^{++}-dependent mechanisms may be involved, including transcription regulation (Spitzer et al. 2002; West et al. 2002), ion channel down-regulation (Klein et al. 2003) and post-translational modifications (Cudmore and Turrigiano 2004), which can be sensitive to the exact pattern and path of Ca^{++} entry (Bito et al. 1997; De Koninck and Schulman 1998; Dolmetsch et al. 1998; Fields 1994; Li et al. 1996). Since we observe no correlation of stimulation-induced activity changes with post inhibitory rebound properties of the neurons studied the question arises of how Ca^{++} influx may play such a crucial role in this phenomenon. We do not have any evidence indicating a possible mechanism but a reduction in intracellular Ca^{++} during hyperpolarizing stimulation may reduce the activation state of some enzymes that maintain the ion channels involved in a high (or low) state of activation. Further experiments are needed to identify the pathways involved in this process.

In conclusion, we suggest that adult STG neurons have a natural predetermined tendency to oscillate. Activity can, however, be regulated in an activity-dependent manner on top of this natural tendency. Only two ionic currents, i_{Ca} and i_K, appear to be involved in both the spontaneous development of oscillations and in activity-induced changes of activity in crab STG neurons. Our dynamic clamp experiments show that regulation of only these two currents is sufficient to produce different changes in activity and may, therefore, provide the mechanisms involved in the homeostatic recovery of pyloric network activity after removal of neuromodulatory input to the ganglion *in situ*.

Acknowledgments: We thank Dr. Farzan Nadim for his extremely useful comments at different stages of this work.

Grants: This work was supported by grants MH 64711 (to J.G.), the NIH Minorities Biomedical Research Support grant GM060826, and National Science Foundation IBN 0090250.

References

Aizenman CD, Akerman CJ, Jensen KR, and Cline HT. Visually driven regulation of intrinsic neuronal excitability improves stimulus detection in vivo. *Neuron* 39: 831-842, 2003.

Bal T, Nagy F, and Moulins M. The pyloric central pattern generator in crustacea: A set of conditional neuronal oscillators. *J Comp Physiol* 163: 715-727, 1988.

Bartos M, Manor Y, Nadim F, Marder E, and Nusbaum MP. Coordination of fast and slow rhythmic neuronal circuits. *J Neurosci* 19: 6650-6660, 1999.

Bito H, Deisseroth K, and Tsien RW. Ca2+-dependent regulation in neuronal gene expression. *Curr Opin Neurobiol* 7: 419-429, 1997.

Brickley SG, Revilla V, Cull-Candy SG, Wisden W, and Farrant M. Adaptive regulation of neuronal excitability by a voltage-independent potassium conductance. *Nature* 409: 88-92, 2001.

Chung JM, Huguenard JR, and Prince DA. Transient enhancement of low-threshold calcium current in thalamic relay neurons after corticectomy. *J Neurophysiol* 70: 20-27, 1993.

Cudmore RH and Turrigiano GG. Long-term potentiation of intrinsic excitability in LV visual cortical neurons. *J Neurophysiol* 92: 341-348, 2004.

Daoudal G and Debanne D. Long-term plasticity of intrinsic excitability: learning rules and mechanisms. *Learn Mem* 10: 456-465, 2003.

Darlington CL, Dutia MB, and Smith PF. The contribution of the intrinsic excitability of vestibular nucleus neurons to recovery from vestibular damage. *Eur J Neurosci* 15: 1719-1727, 2002.

Davis GW and Bezprozvanny I. Maintaining the stability of neural function: a homeostatic hypothesis. *Annu Rev Physiol* 63: 847-869, 2001.

De Koninck P and Schulman H. Sensitivity of CaM kinase II to the frequency of Ca2+ oscillations. *Science* 279: 227-230, 1998.

DeLorme EM, Rabe CS, and McGee R, Jr. Regulation of the number of functional voltage-sensitive Ca++ channels on PC12 cells by chronic changes in membrane potential. *J Pharmacol Exp Ther* 244: 838-843, 1988.

Desai NS, Rutherford LC, and Turrigiano GG. Plasticity in the intrinsic excitability of cortical pyramidal neurons. *Nat Neurosci* 2: 515-520, 1999.

Dolmetsch RE, Xu K, and Lewis RS. Calcium oscillations increase the efficiency and specificity of gene expression. *Nature* 392: 933-936, 1998.

Fields RD. Regulation of neurite outgrowth and immediate early gene expression by patterned electrical stimulation. *Prog Brain Res* 103: 127-136, 1994.

Franklin JL, Fickbohm DJ, and Willard AL. Long-term regulation of neuronal calcium currents by prolonged changes of membrane potential. *J Neurosci* 12: 1726-1735, 1992.

Galante M, Avossa D, Rosato-Siri M, and Ballerini L. Homeostatic plasticity induced by chronic block of AMPA/kainate receptors modulates the generation of rhythmic bursting in rat spinal cord organotypic cultures. *Eur J Neurosci* 14: 903-917, 2001.

Garcia DE, Cavalie A, and Lux HD. Enhancement of voltage-gated Ca2+ currents induced by daily stimulation of hippocampal neurons with glutamate. *J Neurosci* 14: 545-553, 1994.

Golowasch J, Abbott LF, and Marder E. Activity-dependent regulation of potassium currents in an identified neuron of the stomatogastric ganglion of the crab Cancer borealis. *J Neurosci* 19: RC33., 1999a.

Golowasch J, Casey M, Abbott LF, and Marder E. Network stability from activity-dependent regulation of neuronal conductances. *Neural Comput* 11: 1079-1096., 1999b.

Golowasch J and Marder E. Ionic currents of the lateral pyloric neuron of the stomatogastric ganglion of the crab. *J Neurophysiol* 67: 318-331., 1992.

Graubard K and Hartline DK. Voltage clamp analysis of intact stomatogastric neurons. *Brain Res* 557: 241-254, 1991.

Hong SJ and Lnenicka GA. Activity-dependent reduction in voltage-dependent calcium current in a crayfish motoneuron. *J Neurosci* 15: 3539-3547, 1995.

Kilman VL and Marder E. Ultrastructure of the stomatogastric ganglion neuropil of the crab, Cancer borealis. *J Comp Neurol* 374: 362-375, 1996.

Klein JP, Tendi EA, Dib-Hajj SD, Fields RD, and Waxman SG. Patterned electrical activity modulates sodium channel expression in sensory neurons. *J Neurosci Res* 74: 192-198, 2003.

Le Feuvre Y, Fenelon VS, and Meyrand P. Central inputs mask multiple adult neural networks within a single embryonic network. *Nature* 402: 660-664., 1999.

Leao RN, Berntson A, Forsythe ID, and Walmsley B. Reduced low-voltage activated K+ conductances and enhanced central excitability in a congenitally deaf (dn/dn) mouse. *J Physiol* 559: 25-33, 2004.

Li M, Jia M, Fields RD, and Nelson PG. Modulation of calcium currents by electrical activity. *J Neurophysiol* 76: 2595-2607, 1996.

Linsdell P and Moody WJ. Na+ channel mis-expression accelerates K+ channel development in embryonic Xenopus laevis skeletal muscle. *J Physiol* 480 (Pt 3): 405-410, 1994.

Liu Z, Golowasch J, Marder E, and Abbott LF. A model neuron with activity-dependent conductances regulated by multiple calcium sensors. *J Neurosci* 18, 1998.

Luther JA, Robie AA, Yarotsky J, Reina C, Marder E, and Golowasch J. Episodic bouts of activity accompany recovery of rhythmic output by a neuromodulator- and activity-deprived adult neural network. *J Neurophysiol* 90: 2720-2730, 2003.

Marder E, Abbott LF, Turrigiano GG, Liu Z, and Golowasch J. Memory from the dynamics of intrinsic membrane currents. *Proc Natl Acad Sci U S A* 93: 13481-13486, 1996.

Mee CJ, Pym EC, Moffat KG, and Baines RA. Regulation of neuronal excitability through pumilio-dependent control of a sodium channel gene. *J Neurosci* 24: 8695-8703, 2004.

Miller JP and Selverston AI. Mechanisms underlying pattern generation in lobster stomatogastric ganglion as determined by selective inactivation of identified neurons. II. Oscillatory properties of pyloric neurons. *J Neurophysiol* 48: 1378-1391, 1982.

Mizrahi A, Dickinson PS, Kloppenburg P, Fenelon V, Baro DJ, Harris-Warrick RM, Meyrand P, and Simmers J. Long-term maintenance of channel distribution in a central pattern generator neuron by neuromodulatory inputs revealed by decentralization in organ culture. *J Neurosci* 21: 7331-7339, 2001.

Nusbaum MP and Beenhakker MP. A small-systems approach to motor pattern generation. *Nature* 417: 343-350., 2002.

Nusbaum MP and Marder E. A modulatory proctolin-containing neuron (MPN). II. State-dependent modulation of rhythmic motor activity. *J Neurosci* 9: 1600-1607, 1989.

Schulman H, Heist K, and Srinivasan M. Decoding Ca2+ signals to the nucleus by multifunctional CaM kinase. *Prog Brain Res* 105: 95-104, 1995.

Selverston AI, Russell DF, and Miller JP. The stomatogastric nervous system: structure and function of a small neural network. *Prog Neurobiol* 7: 215-290, 1976.

Sharp AA, O'Neil MB, Abbott LF, and Marder E. Dynamic clamp: computer-generated conductances in real neurons. *J Neurophysiol* 69: 992-995, 1993.

Spitzer NC, Kingston PA, Manning TJ, and Conklin MW. Outside and in: development of neuronal excitability. *Curr Opin Neurobiol* 12: 315-323, 2002.

Su H, Sochivko D, Becker A, Chen J, Jiang Y, Yaari Y, and Beck H. Upregulation of a T-type Ca2+ channel causes a long-lasting modification of neuronal firing mode after status epilepticus. *J Neurosci* 22: 3645-3655, 2002.

Thoby-Brisson M and Simmers J. Long-term neuromodulatory regulation of a motor pattern-generating network: maintenance of synaptic efficacy and oscillatory properties. *J Neurophysiol* 88: 2942-2953, 2002.

Thoby-Brisson M and Simmers J. Neuromodulatory inputs maintain expression of a lobster motor pattern- generating network in a modulation-dependent state: evidence from long- term decentralization in vitro. *J Neurosci* 18: 2212-2225, 1998.

Thoby-Brisson M and Simmers J. Transition to endogenous bursting after long-term decentralization requires De novo transcription in a critical time window. *J Neurophysiol* 84: 596-599., 2000.

Turrigiano G, Abbott LF, and Marder E. Activity-dependent changes in the intrinsic properties of cultured neurons. *Science* 264: 974-977, 1994.

Turrigiano G, LeMasson G, and Marder E. Selective regulation of current densities underlies spontaneous changes in the activity of cultured neurons. *J Neurosci* 15: 3640-3652, 1995.

Turrigiano GG and Nelson SB. Homeostatic plasticity in the developing nervous system. *Nat Rev Neurosci* 5: 97-107, 2004.

West AE, Griffith EC, and Greenberg ME. Regulation of transcription factors by neuronal activity. *Nat Rev Neurosci* 3: 921-931, 2002.

Zhang W and Linden DJ. The other side of the engram: experience-driven changes in neuronal intrinsic excitability. *Nat Rev Neurosci* 4: 885-900, 2003.

Figure Legends

Figure 1. *Spontaneous activity and neuronal morphology*. Dissociated STG neurons were photographed and impaled with one electrode at different days in culture. The neurons showed little growth at day 0 and often little even on day 1. **A**. At day 1 in culture this neuron is silent, becomes tonically active by day 4, and develops bursting activity by day 6 with action potentials riding on the slow oscillations of the membrane potential. On day 6 this neuron shows an extensive lamellipodium with many small processes growing at its edges. Arrowheads indicate −53mV. **B**. This neurons shows incipient growth at the end of the neuritic stump on day 1 that grows into a broad lamellipodium by day 6 from which several projections with extensive dendritic processes originate. The neuron is silent on day 1 and begins to generate membrane potential oscillations classified as bursting (high duty cycle) that increases in frequency at day 6. Arrowheads indicate −63mV. **C**. On day 6 this neuron extends two long projections from the original stump (Day 0) and a relatively modest dendritic outgrowth emerging from them. Bursting activity appears immediately after dissociation, becomes silent by day 4 and then resumes bursting by day 6. Arrowheads indicate −66mV. **D**. On day 23 this neuron shows a long neurite with extensive but short branches emerging all along. Recording above the picture shows typical spontaneous plateau potentials observed in 7/13 neurons followed by a plateau potential induced and then terminated early by brief depolarizing and hyperpolarizing current pulses respectively (shown in the trace below). Arrowhead indicates −67mV. Recording below the picture shows characteristic bursting recorded in 6/13 neurons during injection of depolarizing current (bottom trace). Arrowhead indicates −77mV. The baseline of all current traces is 0nA.

Figure 2. *Spontaneous progression of activity and ionic conductances in culture*. **A**. Neurons classified as silent, tonic or bursting were counted on successive days in cell culture and the percentage of each category is plotted as a function of time. A progressive decrease of silent neurons and increase in both tonic and bursting neurons is observed with nearly all neurons expressing bursting (or plateau potentials, see text) after 23 days in culture. **B**. Ca^{++} and high-threshold K^{+} conductance density changes. The changes observed in these conductances are statistically significant (g_{Ca}: $P = 0.047$, n = 65; g_K: P

= 0.002, n = 38). **C**. A, h and leak current conductances changes. g_h was measured at the end of 4sec long hyperpolarizing voltage steps to −120mV. The values were scaled up 10 fold to increase visibility. No statistically significant change in either g_A or g_h could be detected (g_A: P = 0.654, n = 62; g_h: P = 0.313, n = 59). g_{leak} showed a statistically significant increase with time in culture (P = <0.001, n = 139) but this disappeared when the density values were considered (not shown). All statistical comparisons were made using the Kruskal-Wallis One Way ANOVA on Ranks. Data show means ± SD.

Figure 3. *Rhythmic stimulation-induced neuronal activity changes*. Examples of activity transitions resulting from rhythmic stimulation for 45-60 minutes with hyperpolarizing current pulses (see Methods). A total of 50 neurons were recorded in normal *Cancer* saline before (Control) and After stimulation. **A**. *Silent to bursting transition*. In control the neuron was silent. After 60 minutes of rhythmic stimulation the activity changed to rapid oscillations that we classify as bursting because of the high duty cycle. The activity shown was elicited with +0.1nA current injection. Arrowheads indicate −55mV. **B**. *Bursting to tonic transition*. This neuron generated bursts of 2 to 3 action potentials during the depolarizing phase of the membrane potential produced by a +0.4nA current injection (Control). After 60 minutes of stimulation this pattern reversibly changed to tonic firing (After Stim). Reversal took approximately 2 hours of no stimulation. Arrowheads indicate −60mV. **C**. *Tonic to bursting transition*. +0.4nA depolarizing current was used in all traces. Tonic firing is observed before stimulation (Control), and 60 minutes of rhythmic stimulation induced robust bursting (After Stim). The pattern reversed to tonic firing after approximately 2 hours of no stimulation (Reversal). Arrowheads indicate −45mV. **D**. Percentage of neurons (from a total of 50) that changed activity between silent (S), tonic (T) and bursting (B) after 45-60 minutes of rhythmic stimulation. **E**. Voltage changes during the period of hyperpolarizing stimulation used to induce activity changes. Horizontal bars below traces indicate hyperpolarizing current injection. Traces labeled A-C correspond to those cells whose activity states are shown in panels A-C in this figure. The bottom trace corresponds to a bursting cell whose activity did not change as a result of prolonged stimulation. Notice the presence of PIR in this cell and in trace B, but no PIR in traces A and C. **F**. High threshold K^+ conductance

measured at +10mV in normal saline before (grey bars) and after 45-60 minutes of stimulation (black bars) in neurons that showed a clear activity change with patterned stimulation (left; ** $P = 0.005$, n = 6, paired Student t-test) and in neurons that showed no difference in activity pattern (right; $P = 0.375$, n = 6, paired Student t-test).

Figure 4. *Rhythmic stimulation-induced changes in neuronal activity in reduced outward currents*. Neurons were bathed in 20mM TEA to reduce the dominant outward currents. In the presence of TEA 40% of the cells were initially silent and 60% were initially bursting in response to small depolarizing current pulses. **A**. Example of one of the 6/15 neurons that shifted their activity from silent (Control) to bursting (After Stim) upon rhythmic stimulation. Arrowheads indicate –87mV. Current injection: +0.1nA. **B**. Example of one of the 9/15 neurons that show bursting behavior upon depolarization (0.4nA) in control conditions. After rhythmic stimulation the neuron displays bursts with larger amplitude and lower frequency (After Stim). Arrowheads indicate –60mV. Bottom traces in A and B show the depolarizing current steps (baseline = 0nA).

Figure 5. *Effect of patterned activity on ionic currents*. **A**. *Top panel* shows raw traces of high-threshold K^+ currents recorded at +10mV in the presence of 20mM TEA in the bath Before (Control) and After 60 minutes of rhythmic stimulation. *Bottom panel* shows the mean (± SD) I-V relationship of steady state normalized currents recorded and shown as above. $P < 0.001$, n = 6, Two-way ANOVA. **B**. *Top panel* shows typical recordings of a calcium current at 0mV in 20mM TEA plus 0.1μM TTX in *Cancer* saline. The neurons were also TEA and Cs loaded to reduce K^+ currents to a minimum. The transient inward current (Control) increased in amplitude After 30 minutes of rhythmic stimulation. *Bottom panel* shows the I-V plot of mean (± SD) peak normalized i_{Ca} recorded as shown above. $P = 0.002$, n = 7, Two-way ANOVA. **C**. *Top panel* shows raw traces of a typical transient A current elicited at 0mV before (Control) and After 60 minutes stimulation. *Lower panel* shows the I-V plot of the mean (± SD) normalized peak i_A recorded as shown in top panel. $P = 0.944$, n = 7, Two-way ANOVA. Arrowheads in top panels of A-C indicate baseline of 0nA. All currents were normalized by dividing each current value by the current measured at 0mV before stimulation. All currents are leak subtracted.

Figure 6. *Role of Ca^{++} influx on activity-dependent conductance regulation*. **A**. *Top panel* shows a non-inactivating inward Ba^{++} current recorded in a neuron bathed in Ba^{++} saline (Control) that is insensitive to prolonged (45 minutes) rhythmic stimulation (After Stim). *Bottom panel* shows the I-V plot of the steady state mean (± SD) normalized currents as shown in the top panel. $P = 0.668$, n = 5, Two-way ANOVA. **B**. When superfused with normal *Cancer* saline plus 200μM Cd^{++} a low amplitude outward current (*Top panel*, Control) that is insensitive to 60 minutes rhythmic stimulation (After Stim) is recorded. The *lower panel* shows the I-V plot of the mean (± SD) steady state currents as shown in the top panel. $P = 0.973$, n = 5, Two-way ANOVA. Arrowheads in top panels indicate baseline of 0nA. Current values were normalized by the current measured at 0mV before stimulation.

Figure 7. *Dynamic clamp experiments*. Activity changes were elicited by dynamic clamp modifications of the high-threshold K^+ and the Ca^{++} conductance (right panels) comparable to the effects on these conductances of prolonged rhythmic stimulation. Activity was elicited by small depolarizing current injections and depended on the amplitude of the injected current and on the intrinsic properties of the specific neuron recorded. Values above arrows are maximum conductance values in nS of dynamic clamp injected currents. A plus sign corresponds to an increase (and a minus sign to a decrease) in conductance. The two high-threshold K^+ conductance components (transient, gKtr, and sustained, gKst) were varied together. The remaining parameters that specify each current are given in Table 1. **A**. *Top panel*: Activity of a 3 day old neuron during +0.8nA current injection. A switch from silent (Control) to bursting (Dynamic clamp) was induced by increasing gCa and reducing gK. Arrowheads indicate –45mV. *Middle panel*: Activity of a 2 day old neuron (left) during +0.1nA current injection. Activity switched from tonic firing (Control) to bursting (Dynamic clamp) by increasing gCa only. Arrowheads indicate –50mV. *Bottom panel*: Same neuron as in top panel but with slightly larger current injection (+0.9nA) elicited bursting activity. Switching from bursting (Control) to either tonic firing (Dynamic clamp, top) or higher frequency and amplitude bursting (Dynamic clamp, bottom) depended on the gCa level provided the K^+ conductance was reduced. Arrowheads indicate –45mV. **B**. Recordings from a neuron at

day 7 in 20mM extracellular TEA. All traces show activity during +0.4nA current injection. Control amplitude of oscillations (Top left) was markedly increased by reducing both components of g_K and increasing g_{Ca} with dynamic clamp (top right). Stimulating the neuron rhythmically with hyperpolarizing pulses for 20 minutes (bottom left, dynamic clamp off) also markedly increased the amplitude. Dynamic clamp injection (bottom right) of currents with reversed polarity from that used before stimulation greatly reversed the effects of stimulation towards control levels. Arrowheads indicate –60mV.

Table 1. Ionic current parameters used for dynamic clamp experiments.

	τ_m (ms)	τ_h (ms)	$V_{1/2m}$ (mV)	$V_{1/2h}$ (mV)	s_m (mV)	s_h (mV)	q	E_{ion} (mV)
iCa	1	300	–13	–16	–9	+10	1	+100
iK_{St}	100	NA	–20	NA	–9	NA	0	–80
iK_{Tr}	1	70	–23	–34	–4	4	1	–80

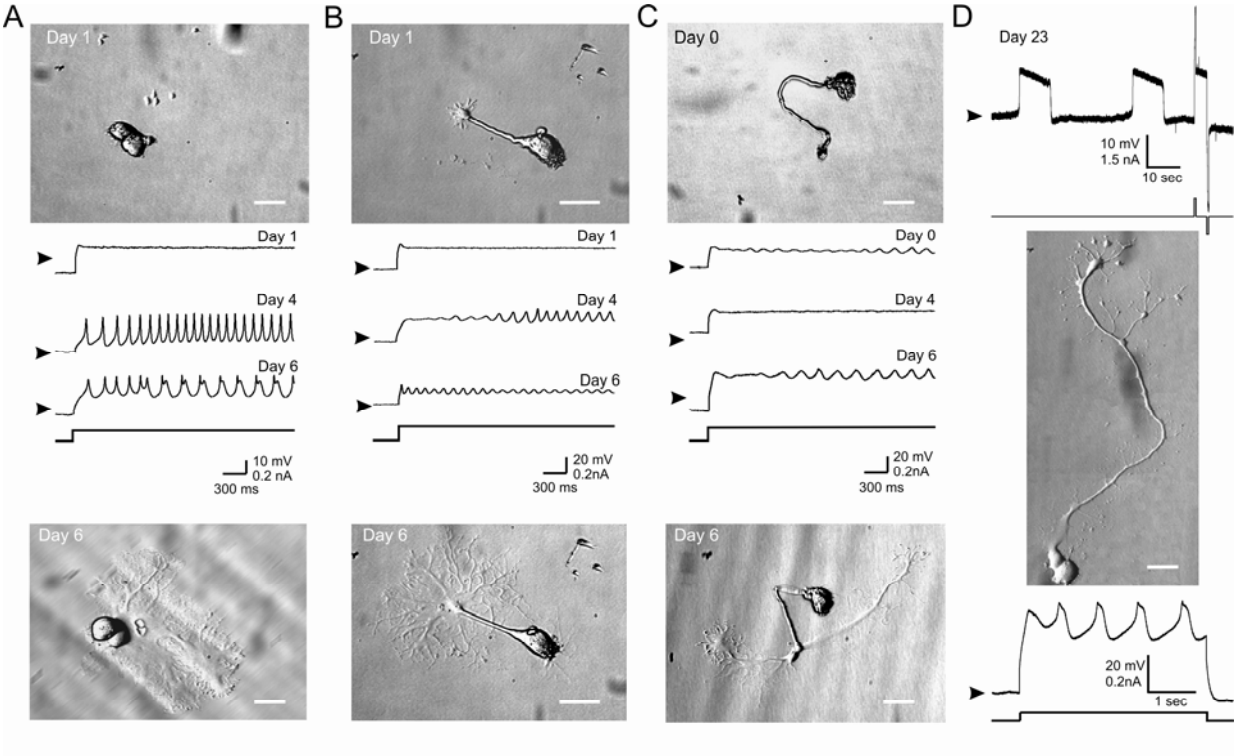

Figure 1. *Spontaneous activity and neuronal morphology*. Dissociated STG neurons were photographed and impaled with one electrode at different days in culture. The neurons showed little growth at day 0 and often little even on day 1. **A**. At day 1 in culture this neuron is silent, becomes tonically active by day 4, and develops bursting activity by day 6 with action potentials riding on the slow oscillations of the membrane potential. On day 6 this neuron shows an extensive lamellipodium with many small processes growing at its edges. Arrowheads indicate –53mV. **B**. This neurons shows incipient growth at the end of the neuritic stump on day 1 that grows into a broad lamellipodium by day 6 from which several projections with extensive dendritic processes originate. The neuron is silent on day 1 and begins to generate membrane potential oscillations classified as bursting (high duty cycle) that increases in frequency at day 6. Arrowheads indicate –63mV. **C**. On day 6 this neuron extends two long projections from the original stump (Day 0) and a relatively modest dendritic outgrowth emerging from them. Bursting activity appears immediately after dissociation, becomes silent by day 4 and then resumes bursting by day 6. Arrowheads indicate –66mV. **D**. On day 23 this neuron shows a long neurite with extensive but short branches emerging all along. Recording above the picture shows typical spontaneous plateau potentials observed in 7/13 neurons followed by a plateau potential induced and then terminated early by brief depolarizing and hyperpolarizing current pulses respectively (shown in the trace below). Arrowhead indicates –67mV. Recording below the picture shows characteristic bursting recorded in 6/13 neurons during injection of depolarizing current (bottom trace). Arrowhead indicates –77mV. The baseline of all current traces is 0nA.

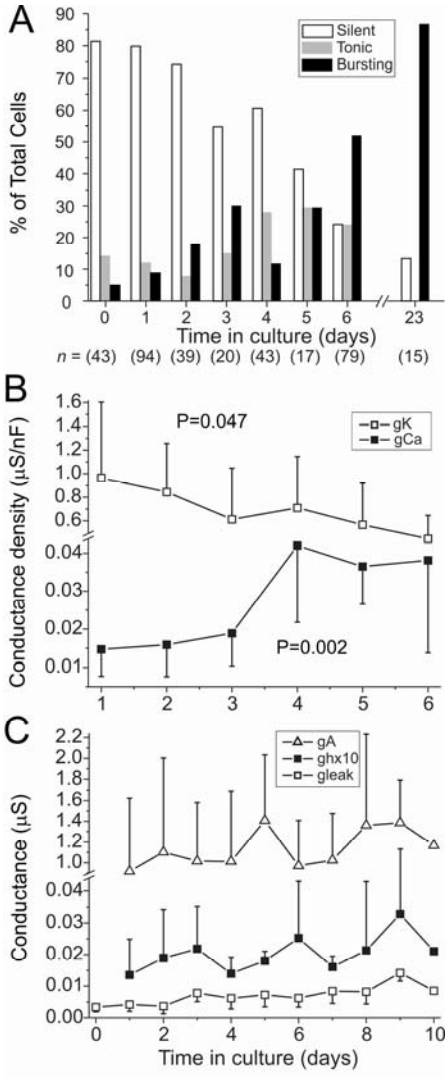

Figure 2. *Spontaneous progression of activity and ionic conductances in culture*. **A**. Neurons classified as silent, tonic or bursting were counted on successive days in cell culture and the percentage of each category is plotted as a function of time. A progressive decrease of silent neurons and increase in both tonic and bursting neurons is observed with nearly all neurons expressing bursting (or plateau potentials, see text) after 23 days in culture. **B**. Ca^{++} and high-threshold K^{+} conductance density changes. The changes observed in these conductances are statistically significant (g_{Ca}: $P = 0.047$, n = 65; g_K: $P = 0.002$, n = 38). **C**. A, h and leak current conductances changes. g_h was measured at the end of 4sec long hyperpolarizing voltage steps to −120mV. The values were scaled up 10 fold to increase visibility. No statistically significant change in either g_A or g_h could be detected (g_A: $P = 0.654$, n = 62; g_h: $P = 0.313$, n = 59). g_{leak} showed a statistically significant increase with time in culture ($P = <0.001$, n = 139) but this disappeared when the density values were considered (not shown). All statistical comparisons were made using the Kruskal-Wallis One Way ANOVA on Ranks. Data show means ± SD.

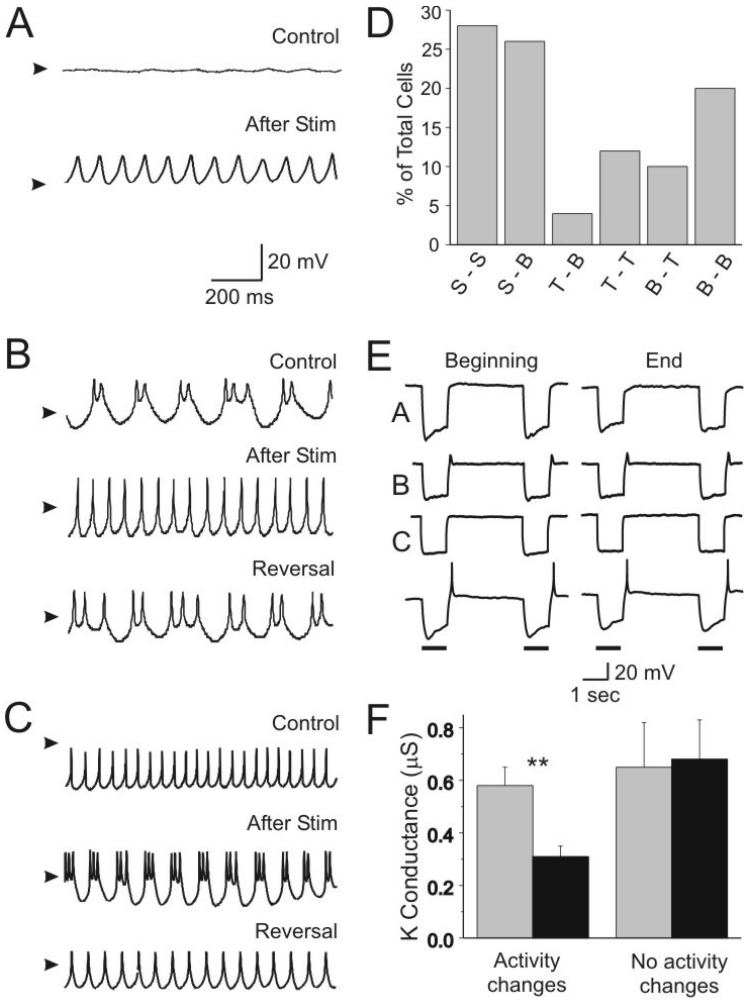

Figure 3. *Rhythmic stimulation-induced neuronal activity changes*. Examples of activity transitions resulting from rhythmic stimulation for 45-60 minutes with hyperpolarizing current pulses (see Methods). A total of 50 neurons were recorded in normal *Cancer* saline before (Control) and After stimulation. **A**. *Silent to bursting transition.* In control the neuron was silent. After 60 minutes of rhythmic stimulation the activity changed to rapid oscillations that we classify as bursting because of the high duty cycle. The activity shown was elicited with +0.1nA current injection. Arrowheads indicate –55mV. **B**. *Bursting to tonic transition*. This neuron generated bursts of 2 to 3 action potentials during the depolarizing phase of the membrane potential produced by a +0.4nA current injection (Control). After 60 minutes of stimulation this pattern reversibly changed to tonic firing (After Stim). Reversal took approximately 2 hours of no stimulation. Arrowheads indicate –60mV. **C**. *Tonic to bursting transition.* +0.4nA depolarizing current was used in all traces. Tonic firing is observed before stimulation (Control), and 60 minutes of rhythmic stimulation induced robust bursting (After Stim). The pattern reversed to tonic firing after approximately 2 hours of no stimulation (Reversal). Arrowheads indicate –45mV. **D**. Percentage of neurons (from a total of 50) that changed activity between silent (S), tonic (T) and bursting (B) after 45-60 minutes of rhythmic stimulation. **E**. Voltage changes during the period of hyperpolarizing stimulation used to induce activity changes. Horizontal bars below traces indicate hyperpolarizing current injection. Traces labeled A-C correspond to those cells whose activity states are shown in panels A-C in this figure. The bottom trace corresponds to a bursting cell whose activity did not change as a result of prolonged stimulation. Notice the presence of PIR in this cell and in trace B, but no PIR in traces A and C. **F**. High threshold K^+ conductance measured at +10mV in normal saline before (grey bars) and after 45-60 minutes of stimulation (black bars) in neurons that showed a clear activity change with patterned stimulation (left; ** $P = 0.005$, n = 6, paired Student t-test) and in neurons that showed no difference in activity pattern (right; $P = 0.375$, n = 6, paired Student t-test).

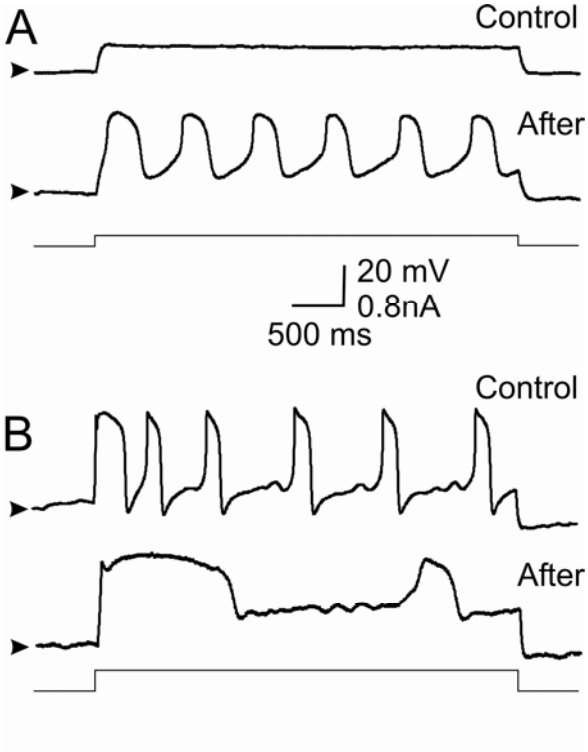

Figure 4. *Rhythmic stimulation-induced changes in neuronal activity in reduced outward currents*. Neurons were bathed in 20mM TEA to reduce the dominant outward currents. In the presence of TEA 40% of the cells were initially silent and 60% were initially bursting in response to small depolarizing current pulses. **A**. Example of one of the 6/15 neurons that shifted their activity from silent (Control) to bursting (After Stim) upon rhythmic stimulation. Arrowheads indicate –87mV. Current injection: +0.1nA. **B**. Example of one of the 9/15 neurons that show bursting behavior upon depolarization (0.4nA) in control conditions. After rhythmic stimulation the neuron displays bursts with larger amplitude and lower frequency (After Stim). Arrowheads indicate –60mV. Bottom traces in A and B show the depolarizing current steps (baseline = 0nA).

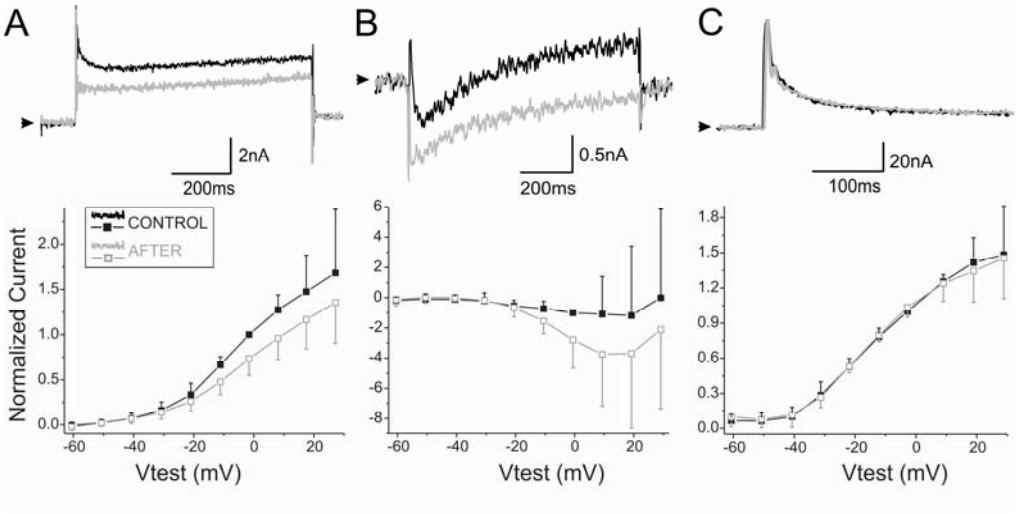

Figure 5. *Effect of patterned activity on ionic currents.* **A**. *Top panel* shows raw traces of high-threshold K^+ currents recorded at +10mV in the presence of 20mM TEA in the bath Before (Control) and After 60 minutes of rhythmic stimulation. *Bottom panel* shows the mean (± SD) I-V relationship of steady state normalized currents recorded and shown as above. $P < 0.001$, n = 6, Two-way ANOVA. **B**. *Top panel* shows typical recordings of a calcium current at 0mV in 20mM TEA plus 0.1µM TTX in *Cancer* saline. The neurons were also TEA and Cs loaded to reduce K^+ currents to a minimum. The transient inward current (Control) increased in amplitude After 30 minutes of rhythmic stimulation. *Bottom panel* shows the I-V plot of mean (± SD) peak normalized i_{Ca} recorded as shown above. $P = 0.002$, n = 7, Two-way ANOVA. **C**. *Top panel* shows raw traces of a typical transient A current elicited at 0mV before (Control) and After 60 minutes stimulation. *Lower panel* shows the I-V plot of the mean (± SD) normalized peak i_A recorded as shown in top panel. $P = 0.944$, n = 7, Two-way ANOVA. Arrowheads in top panels of A-C indicate baseline of 0nA. All currents were normalized by dividing each current value by the current measured at 0mV before stimulation. All currents are leak subtracted.

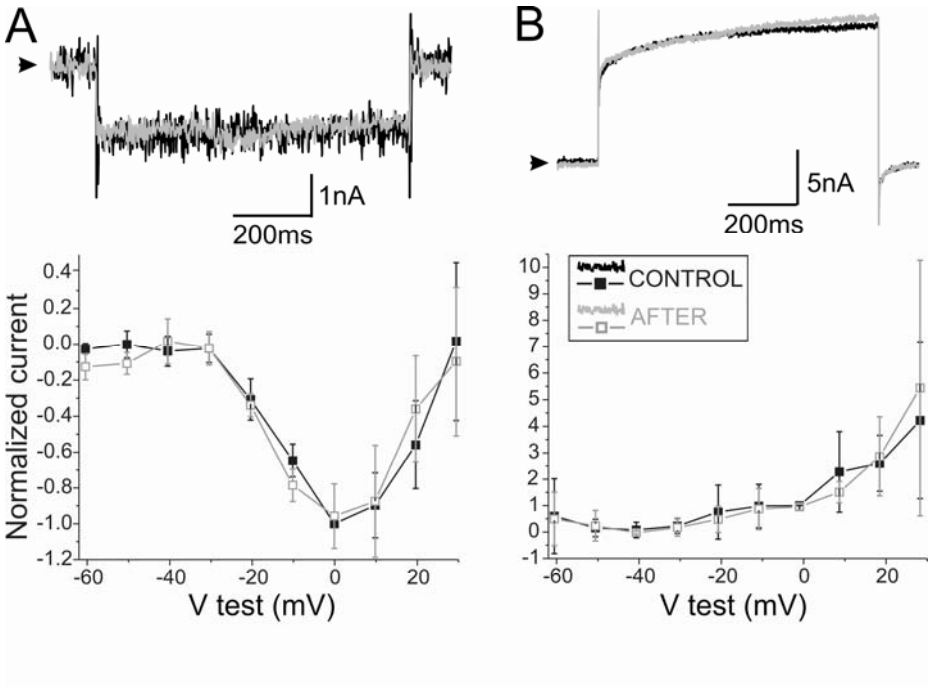

Figure 6. *Role of Ca^{++} influx on activity-dependent conductance regulation*. **A**. *Top panel* shows a non-inactivating inward Ba^{++} current recorded in a neuron bathed in Ba^{++} saline (Control) that is insensitive to prolonged (45 minutes) rhythmic stimulation (After Stim). *Bottom panel* shows the I-V plot of the steady state mean (± SD) normalized currents as shown in the top panel. $P = 0.668$, n = 5, Two-way ANOVA. **B**. When superfused with normal *Cancer* saline plus 200µM Cd^{++} a low amplitude outward current (*Top panel*, Control) that is insensitive to 60 minutes rhythmic stimulation (After Stim) is recorded. The *lower panel* shows the I-V plot of the mean (± SD) steady state currents as shown in the top panel. $P = 0.973$, n = 5, Two-way ANOVA. Arrowheads in top panels indicate baseline of 0nA. Current values were normalized by the current measured at 0mV before stimulation.

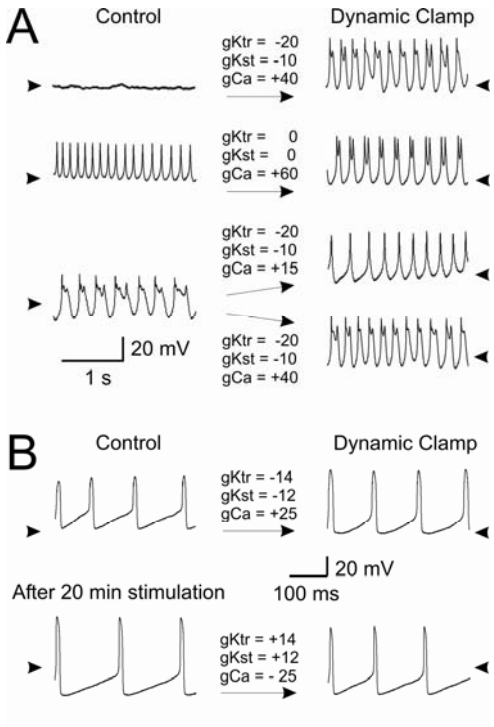

Figure 7. *Dynamic clamp experiments*. Activity changes were elicited by dynamic clamp modifications of the high-threshold K^+ and the Ca^{++} conductance (right panels) comparable to the effects on these conductances of prolonged rhythmic stimulation. Activity was elicited by small depolarizing current injections and depended on the amplitude of the injected current and on the intrinsic properties of the specific neuron recorded. Values above arrows are maximum conductance values in nS of dynamic clamp injected currents. A plus sign corresponds to an increase (and a minus sign to a decrease) in conductance. The two high-threshold K^+ conductance components (transient, gKtr, and sustained, gKst) were varied together. The remaining parameters that specify each current are given in Table 1. **A**. *Top panel*: Activity of a 3 day old neuron during +0.8nA current injection. A switch from silent (Control) to bursting (Dynamic clamp) was induced by increasing gCa and reducing gK. Arrowheads indicate –45mV. *Middle panel*: Activity of a 2 day old neuron (left) during +0.1nA current injection. Activity switched from tonic firing (Control) to bursting (Dynamic clamp) by increasing gCa only. Arrowheads indicate –50mV. *Bottom panel*: Same neuron as in top panel but with slightly larger current injection (+0.9nA) elicited bursting activity. Switching from bursting (Control) to either tonic firing (Dynamic clamp, top) or higher frequency and amplitude bursting (Dynamic clamp, bottom) depended on the gCa level provided the K^+ conductance was reduced. Arrowheads indicate –45mV. **B**. Recordings from a neuron at day 7 in 20mM extracellular TEA. All traces show activity during +0.4nA current injection. Control amplitude of oscillations (Top left) was markedly increased by reducing both components of g_K and increasing g_{Ca} with dynamic clamp (top right). Stimulating the neuron rhythmically with hyperpolarizing pulses for 20 minutes (bottom left, dynamic clamp off) also markedly increased the amplitude. Dynamic clamp injection (bottom right) of currents with reversed polarity from that used before stimulation greatly reversed the effects of stimulation towards control levels. Arrowheads indicate –60mV.